Heliyon 10 (2024) e29779

Contents lists available at ScienceDirect

Heliyon

journal homepage: www.cell.com/heliyon

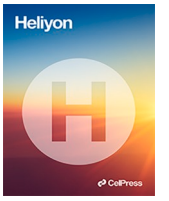

Review article

Magnetic resonance imaging findings in central nervous system tuberculosis: A pictorial review

Prajwal Dahal [a,*], Sabina Parajuli [b]

[a] Department of Radiology and Imaging, Grande International Hospital, Kathmandu, Nepal
[b] Resident PGY-1 Pathology, Department of Pathology, Bir Hospital, Kathmandu, Nepal

ARTICLE INFO

Keywords:
Central nervous system (CNS)
Tuberculosis
Magnetic resonance imaging (MRI)
Proton magnetic resonance spectroscopy (PMRS)
Magnetization transfer ratio (MTR)
Rich foci

ABSTRACT

Central nervous system (CNS) tuberculosis is a post-primary form of tuberculosis. It has high mortality and morbidity rates despite early diagnosis and treatment. CNS tuberculosis can manifest as subacute/chronic meningitis, parenchymal tuberculous lesions, and spinal tuberculosis. Hematogenous spread of tuberculous bacilli to the brain results in the development of so called "rich foci" on the pial surface, ependyma, and grey-white matter junction. Rupture of these "rich foci" into the subarachnoid space triggers an intense granulomatous inflammatory reaction. Tuberculous meningitis can manifest as leptomeningitis or pachymeningitis. Intracranial parenchymal tuberculous lesions may present as tuberculoma, tuberculous abscess, cerebritis, rhombencephalitis, and encephalopathy, with atypical presentations not uncommon. Complications of CNS tuberculosis encompass hydrocephalus, syrinx formation, vasculitis, infarcts, neuritis, and enduring neurological deficits. Post-contrast 3D fluid-attenuated inversion recovery (FLAIR) and post-contrast T1 spin-echo sequences excel in detecting tuberculous meningitis compared to other conventional magnetic resonance imaging (MRI) sequences. In proton magnetic resonance spectroscopy (PMRS), the presence of a lipid peak at 1.3 ppm is indicative of tuberculous lesions. Magnetization transfer (MT) imaging enhances the detection of tuberculous lesions, as the magnetization transfer ratio (MTR) of tuberculous pathologies, owing to their high lipid content, is lower than that in bacterial or fungal pathologies and higher than that in viral pathologies. This review article delves into the various typical and atypical imaging presentations of CNS tuberculosis in MRI, along with recent advances in imaging techniques.

1. Introduction

Tuberculosis (TB) is caused by an acid-fast bacillus, mycobacterium tuberculosis [1]. It primarily infects the lungs but can spread to almost every organ via hematogenous route [2]. Estimated 0.6 million people died in South Asia because of tuberculosis in 2020 [3]. Tuberculosis is a reemerging disease in Western countries because of a surge in acquired immunodeficiency syndrome (AIDS), global migration, overcrowding, and multidrug resistance (MDR) mycobacterium [4,5].

Mycobacterium tuberculosis is responsible for 5.9 % of all community-acquired CNS infections worldwide [6]. According to the center for disease control, meningeal tuberculosis accounted for 3.5 % of all extrapulmonary tuberculosis in the year 2021 [7]. It comprises of 10 % of all tuberculosis cases and 20 % of TB cases in immunocompromised patients [8]. Early detection of the disease

* Corresponding author.
E-mail address: meprajwal7@gmail.com (P. Dahal).

https://doi.org/10.1016/j.heliyon.2024.e29779
Received 27 October 2023; Received in revised form 13 April 2024; Accepted 15 April 2024
Available online 18 April 2024
2405-8440/© 2024 The Author(s). Published by Elsevier Ltd. This is an open access article under the CC BY-NC-ND license (http://creativecommons.org/licenses/by-nc-nd/4.0/).

helps in prevention of associated mortality and morbidity. 15–40 % of patients with CNS tuberculosis die or become permanently disabled despite early diagnosis and aggressive treatment [9]. Imaging, particularly magnetic resonance imaging (MRI), is the investigation of choice for diagnosis and follow-up of CNS tuberculosis.

2. Pathology

Inhalation of mycobacterium tuberculosis into alveolar space results in primary tuberculous infection [10]. CNS tuberculosis is caused due to hematogenous spread of the mycobacterium from lungs to the subpial, subependymal region, brain parenchyma, and meninges to form mycobacterium rich foci called "rich foci" [11]. The "rich foci" rupture to start an intense cytokine-mediated inflammatory reaction [12]. Exudates of the inflammatory reaction are accumulated in basal cisterns and meninges. The structures in and around the basal cisterns are enveloped by inflammatory exudates. Inflammation of arteries and nerves in basal cisterns can cause vasculitis and neuritis. Vasculitis can subsequently lead to infarcts. Cranial nerve palsies occur due to neuritis. Hydrocephalus is often the initial manifestation of tuberculous meningitis. Usually, communicating hydrocephalus occurs in the beginning due to blockage of cerebrospinal fluid (CSF) resorption in basal cisterns by the inflammatory exudates. Unruptured rich foci lead to the formation of tuberculomas [12]. Few cases of intracranial tuberculosis due to direct spread from paranasal sinuses, mastoid air cells, and calvaria have also been reported [13,14].

3. Imaging

MRI is the imaging modality of choice for suspected CNS tuberculosis, as it can detect changes in all forms of CNS tuberculosis during the early stages [15]. It can accurately demonstrate complications such as infarction, hydrocephalus, and vasculitis with a high degree of precision. MRI has better specificity for detection of intracranial tuberculous pathologies than CT [15,16]. MRI plays a crucial role in prognosticating patients with CNS tuberculosis. Presence of large, multiple lesions in eloquent locations, marked perilesional edema, hydrocephalus and infarcts are predictors of bad prognosis [17].

While MRI is considered superior, contrast-enhanced computed tomography (CT) also plays a crucial role, especially in imaging unstable patients and those with a low Glasgow Coma Scale (GCS) score. In unstable patients, CT allows for quick image acquisition [18]. Additionally, if a patient is irritable, motion artifacts may reduce the quality of MRI images. CT, with its rapid imaging capabilities, helps eliminate motion artifacts [19]. In this review article, we will discuss various typical and atypical imaging presentations of intracranial tuberculosis and the complications of each form. We will also discuss the closest differential of each type and imaging features to differentiate them from tuberculosis in both conventional MRI sequences and recent advances.

4. MRI protocol

For patients undergoing MRI for suspected intracranial tuberculosis, following sequences are acquired in our hospital.

a) T1 axial – from the vertex to the base of skull
b) T2 axial – from the vertex to the base of skull
c) Fluid Attenuation Inversion Recovery (FLAIR) axial– from the vertex to the base of skull
d) Diffusion-weighted images (DWI) and Apparent Diffusion Coefficient (ADC) axial– from the vertex to the base of skull
e) Susceptibility weighted images (SWI) axial – from the vertex to the base of skull
f) Pre- and post-contrast 3D T1 gradient echo images.
g) Pre- and post-contrast 3D FLAIR images.
h) Post-contrast fat saturated spin echo T1 images- Axial, Coronal, and Sagittal planes.
i) Pre- and post-contrast magnetization transfer (MT) T1 axial images- from the vertex to the base of skull.
j) Proton MRI Spectroscopy (PMRS) [Short TE (20–35 ms), 2D single voxel acquisition]
k) Magnetic Resonance Angiography (MRA) and Magnetic Resonance Venography (MRV) if vasculitis is suspected.

In suspected spine tuberculosis, following sequences of whole spine are done.

a) T1, T2- in axial, and sagittal planes
b) Short tau Inversion Recovery (STIR) sequence - in sagittal, and coronal planes
c) T1 fat-saturated pre- and post-contrast -in axial, sagittal, and coronal planes.

Due to the high patient volume at our hospital, we typically acquire basic brain sequences, including post-contrast 3D FLAIR, post-contrast 3D T1, and PMRS for practical purposes. Additional sequences are obtained as necessary, with the entire process usually lasting 20–25 min. For spine imaging, we begin by obtaining sagittal images of the entire spine. If abnormalities are detected, a dedicated scan of the affected area is performed, taking approximately 45 min. A dedicated scan of the entire spine is conducted if there is suspicion of conditions such as tuberculous arachnoiditis, transverse myelitis, or spinal cord abscess, which typically takes about 1 h and 15 min.

Conventional T1, T2, and FLAIR sequences help in defining anatomy. T2 images are sensitive for detecting tuberculomas. Pre-contrast FLAIR images are important for detecting perilesional edema, hydrocephalus, and periventricular CSF ooze. Pre-contrast

3D FLAIR images are sensitive for detecting basal meningeal and cisternal exudates. Post-contrast 3D FLAIR is considered more sensitive than post-contrast 3D T1 gradient echo image for detecting basal meningeal and cisternal exudates. This is because there is no enhancement of blood vessels in post- contrast 3D FLAIR and the meningeal enhancement can be easily detected [20]. T1 spin echo sequences are preferred over T1 gradient echo images for post-contrast 3D sequences due to better meningeal enhancement [21]. Diffusion-weighted images can detect the presence of acute/subacute infarcts due to tuberculous vasculitis. SWI images can detect hemorrhage and calcification. Hemorrhage is rare in tuberculous lesions. Few cases of cortical venous thrombosis and hemorrhagic infarcts due to tuberculosis have been reported [22,23]. Calcifications can occur in tuberculous granulomas which can be detected in SWI images. Pre- and post-contrast 3D T1 gradient echo images are necessary for the demonstration of enhancement of meningeal and basal exudates. We routinely acquire fat saturated spin echo T1 post-contrast images in all planes to demonstrate contrast enhancement of meninges and rim of tuberculomas. Pre- and post-contrast magnetization transfer T1 images are considered more sensitive than conventional T1 sequences for detecting tuberculous meningitis. The MT images are useful in subtle or early meningitis. The rim of tuberculomas and abnormal meninges are hyperintense in T1 pre-contrast MT images [24]. Post-contrast MT images show better enhancement of meninges and basal exudates. The magnetization transfer ratio (MTR) of the meninges in tuberculous meningitis is lower than that of fungal and pyogenic meningitis and higher than that of viral meningitis owing to the high lipid content of tuberculous bacilli. MTR helps in predicting the cause of meningitis. Proton magnetic resonance imaging spectroscopy (PMRS) can detect lipid contents in tuberculomas. Long TE (270–288 ms), intermediate TE (135–144 ms) as well as short TE (20–35 ms) PMRS can be done. However, short TE PMRS has better resolution because of high signal to noise ratio. We acquire short TE 2D single voxel PMRS routinely. A lipid peak at 1.3 ppm is seen in tuberculomas. Single voxel spectroscopy technique with the voxel in the central caseous/necrotic part gives better results [25,26]. In the case of tuberculous abscess with variegated appearance, owing to the presence of high cellularity, a choline peak at 3.2 ppm may be present in addition to the lipid peak if the voxel is placed in enhancing wall.

MRA and MRV should be performed if vascular complications are suspected. A recent MRI breakthrough, high-resolution vessel wall imaging (HR-VWI), enables submillimeter assessment of arterial walls, aiding in diagnosing tuberculous arteritis [27]. Hypotheses suggest that tuberculous vasculitis occurs due to infiltrative, proliferative, necrotizing, and autoimmune pathology. HR-VWI exhibits nodular or smooth segmental wall enhancement with or without stenosis [28]. Despite its significance in early tuberculous arteritis identification, HR-VWI has limitations, including extended scanning durations, heightening the risk of motion artifacts and potential discomfort for patients in acute phases [15].

5. Imaging features of CNS tuberculosis in MRI

Different forms of CNS tuberculosis are enlisted in Table 1.
Intracranial tuberculosis: Intracranial tuberculosis can be present either in meningeal form or parenchymal form.

A) Meningeal tuberculosis: Meningeal tuberculosis (TBM) can either be present in the leptomeningeal form or pachymeningeal form.

1) Tuberculous leptomeningitis (Figs. 2A-2F and 3A-3F): This is the most common and devastating form of intracranial tuberculosis [27,28]. It accounts for 70–80 % of all forms of neurotuberculosis [29]. In HIV-infected patients, tuberculosis is more likely to produce meningitis. In a study of 2205 patients with TB, 10 % of HIV-positive patients had TB meningitis compared to only 2 % of patients without HIV infection [30]. The imaging features are seen because of the intense granulomatous inflammatory reaction elicited by the rupture of 'rich foci' in subarachnoid space [11]. In plain MRI, basal exudates may be seen as a high signal in FLAIR. There may be effacement of basal cisterns with dirty CSF in T1 weighted images due to the presence of communicating hydrocephalus. Hydrocephalus may be the only finding in plain MRI. Non-communicating hydrocephalus may be seen in later stages due to intraventricular exudates and adhesions [5]. In post-contrast T1 images, there is diffuse thickening and enhancement of leptomeninges and exudates in basal meninges and cisterns [26]. The basal exudates are seen more in peri mesencephalic cisterns including quadrigeminal cisterns, ambient cisterns, crural cisterns, interpeduncular cisterns, suprasellar cisterns, bilateral middle cerebral arteries cisterns, bilateral sylvian cisterns, peri pontine and peri medullary cisterns [10,31]. Because of the predilection of tuberculous meningitis to affect the basal region and cisterns, the involvement of cranial nerves and arteries is not uncommon [32]. Optochiasmatic arachnoiditis is a serious complication of tuberculous meningitis and is

Table 1
Different forms of CNS tuberculosis.

Intracranial Tuberculosis	Spinal Tuberculosis	Miscellaneous
A) Meningeal Form:	1) Extradural Form	1) Tuberculous Hypophysitis
1) Leptomeningitis	2) Intradural Extramedullary Form	2) Orbital Tuberculosis
2) Pachymeningitis	3) Intramedullary Form	3) Tuberculous otitis media and temporal bone tuberculosis
B) Parenchymal Form		4) Tuberculous osteomyelitis of calvarial bone.
1) Tuberculoma		5) Tuberculous osteomyelitis of base of skull
2) Disseminated/Miliary Tuberculomas		
3) Tuberculous abscess		
4) Tuberculous cerebritis		
5) Rhombencephalitis		
6) Encephalopathy		

Table 2
MRI features of different stages of tuberculoma.

Stage of tuberculoma	T1 Weighted Image	T2 Weighted Image	FLAIR	DWI	SWI/GRE	T1 Post Contrast
Non-Caseating Granuloma (Fig. 7A-7F)	Iso to low signal lesion	High signal lesion	No suppression	No diffusion restriction	No blooming	Homogeneous disc enhancement (high signal in post contrast images)
Caseating Solid Granuloma (Figs. 5A-5E, 6A-6D, 7A-7F)	Iso to low signal lesion	Markedly low signal lesion	No suppression	No diffusion restriction	No blooming	Disc/ring enhancement
Caseating Granuloma with central liquefaction	Iso to low signal lesion	High signal central portion with low signal rim	Partial suppression of signal	May show central diffusion restriction	Subtle but complete peripheral blooming	Ring enhancement
Calcified Granuloma	Iso to low signal lesion	Low signal lesion	No suppression	No diffusion restriction	Blooming present	No enhancement/subtle ring enhancement

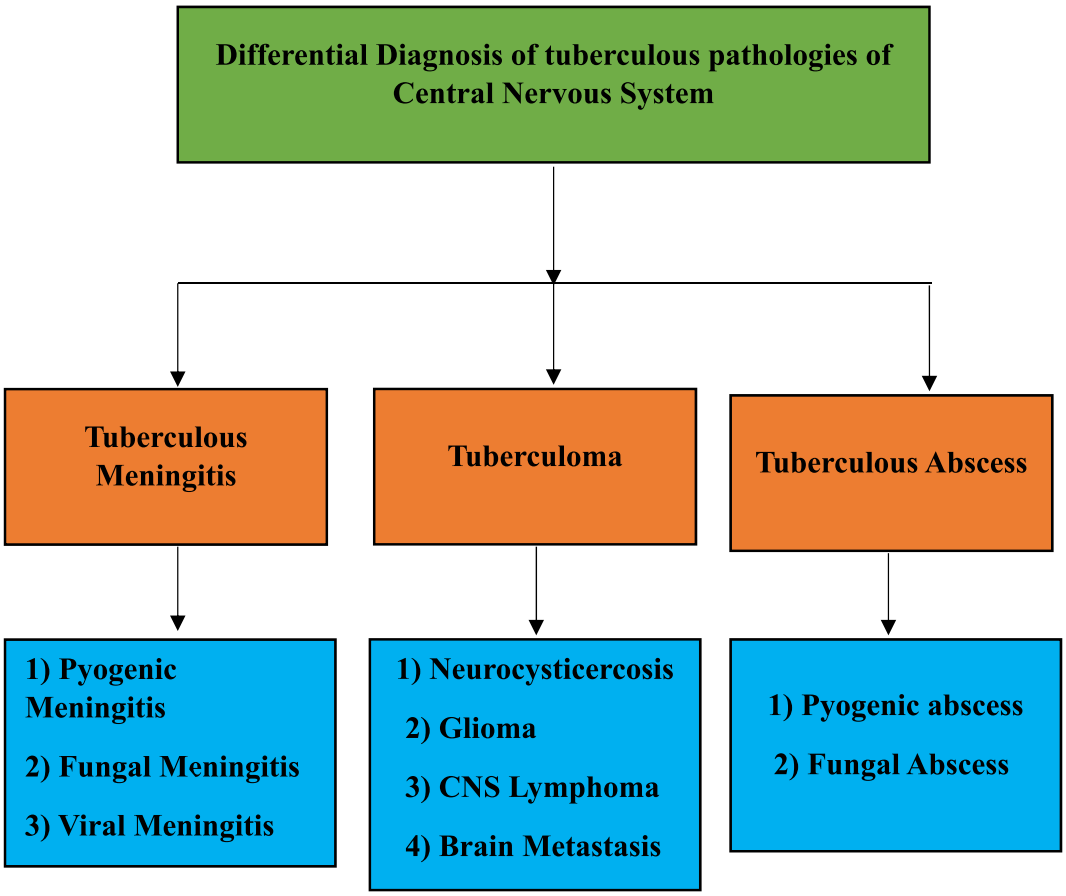

Fig. 1. Flowchart showing differential diagnosis of CNS tuberculous pathologies.

often associated with vision loss [33], infarcts, and non-communicating hydrocephalus [34]. It is characterized by inflammation of the arachnoid membrane in the region of the optic chiasm. In MRI, optochiasmatic arachnoiditis can be diagnosed if there is thickening, enhancement, or distortion of the intracranial optic nerve or optic chiasm, or the surrounding cisterns (cisternal and suprasellar spaces surrounding the optic chiasma). Exudates and tuberculomas can be present in the cerebrospinal fluid (CSF) spaces around the optic nerve and optic chiasma [33]. Non-communicating hydrocephalus and infarcts may also be present.

Linear enhancement of meninges seen in more than two contagious slices is considered abnormal. Other abnormal meningeal enhancement patterns include nodular enhancement, asymmetrical enhancement on two sides, double and triple lines along bilateral

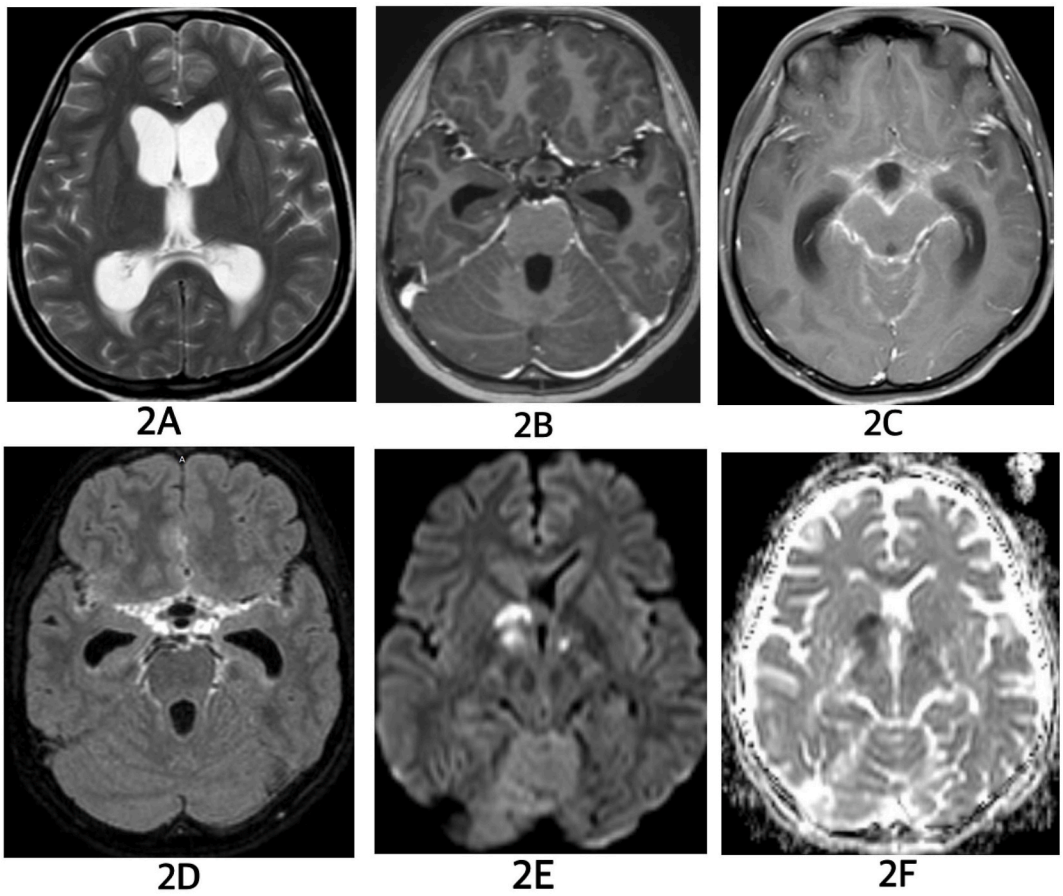

Fig. 2. MRI of a 20 years old female with HIV negative status showing leptomeningeal TBM with infarct. Axial T2 (2A) shows hydrocephalus. Post contrast (PC) 3D T1 gradient echo (2B) reveals leptomeningeal enhancement in peri pontine region. PC T1 spin echo (2C) highlights enhancement at interpeduncular, sylvian and perimesencephalic cisterns. PC 3D FLAIR (2D) displays meningeal enhancement better than PC 3D T1 gradient echo and comparable to PC T1 spin echo. DWI and ADC (2E, 2F) show acute infarct in right globus pallidus and bilateral subthalami.

middle cerebral arteries, enhancement in the infundibular recess of the third ventricle, and enhancement with ill-defined edges [35,36]. In addition, ependymitis/ventriculitis may be seen as an enhancement of the ependymal lining (Fig. 6A-6D). This occurs due to intraventricular rupture of infective focus [37]. Choroid plexitis may be seen as hyperenhancement and exudates in the choroid plexus [38]. Exudates along the vessels result in vasculitis and infarcts. Typically, small and medium-sized vessels are involved. The lenticulostriate and thalamo-perforating vessels are mostly involved resulting in infarcts in the gangliothalamic region [39].

2) Tuberculous Pachymeningitis (Fig. 4A-4F): This is an uncommon manifestation of tuberculous meningitis. Tuberculous pachymeningitis occurs as sequelae of acute or chronic leptomeningitis. In MRI, pachymeningeal lesions demonstrate iso or low signal on T1 and T2 weighted images, and intense and homogeneous contrast enhancement [40]. The distribution pattern can be focal or diffuse, presenting with an en plaque configuration and associated with vasculitis, cranial nerve palsy, and ischemia. FLAIR sequence is particularly important for the detection of dural thickening. The thickened dura shows a high signal in FLAIR (41). If other features of CNS tuberculosis are present along with pachymeningeal thickening, there should be no diagnostic confusion. However, isolated pachymeningeal thickening creates a diagnostic dilemma. Differential diagnosis of isolated pachymeningeal thickening is neurosarcoidosis, en-plaque meningioma, idiopathic hypertrophic pachymeningitis, autoimmune diseases with CNS involvement (Granulomatosis with polyangiitis, rheumatoid arthritis) [5,41].

B) Parenchymal tuberculosis: Parenchymal tuberculosis can present as tuberculoma, disseminated/miliary tuberculomas, tuberculous abscess, tuberculous cerebritis, rhombencephalitis, or encephalopathy.

1) Tuberculoma: Unruptured rich foci develop as tuberculomas [12]. Tuberculomas accompany TB meningitis in 10 % of patients and are multiple in a third of patients [30]. They are more common in the pediatric age group. It usually occurs at the grey-white matter junction and periventricular location due to the narrowing of the caliber of the blood vessels at this level. However; parenchymal, cisternal, and gangliothalamic locations are not rare. The rare site of tuberculoma is the cavernous sinus, sphenoid sinus, and along optic nerves. MRI features of tuberculoma depend upon the stage of tuberculoma [42,43]. In adults supratentorial location is

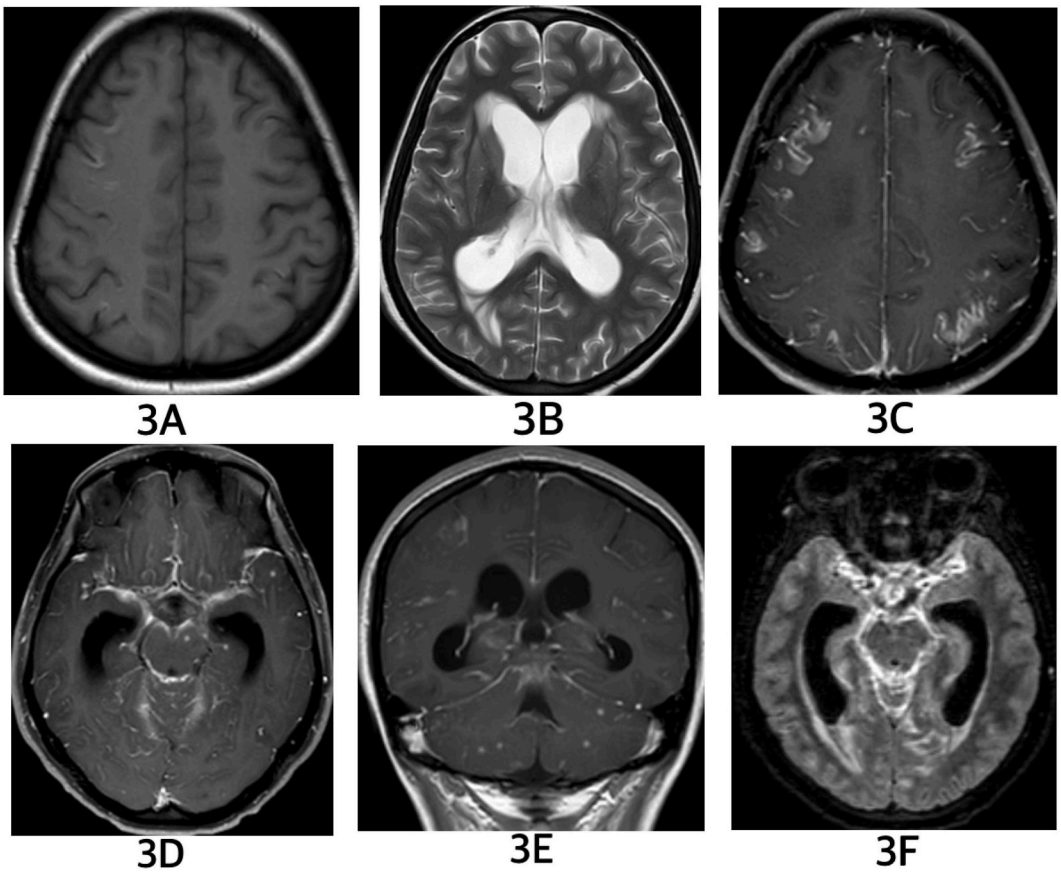

Fig. 3. MRI of a 45 years old female with HIV negative status showing leptomeningeal TBM with miliary tuberculomas. Axial T1 without contrast (3A) shows gyriform high signal in right frontal and bilateral parietal lobes. T2 (3B) reveals hydrocephalus. PC T1 (3C) demonstrates gyriform enhancement in bilateral frontal and parietal lobes, and leptomeningeal enhancement in peri mesencephalic cisterns (3D). Miliary tuberculomas are seen in left cerebral peduncle and left temporal lobe (3D). Coronal PC T1 (3E) shows leptomeningeal enhancement along tentorium cerebelli and miliary tuberculomas in bilateral cerebellum. Axial post-contrast 3D FLAIR (3F) reveals exudates and leptomeningeal enhancement along basal cerebral cisterns.

common and in children, infratentorial location is common [44]. There are 4 stages of tuberculoma [5,45]. MRI features of different stages of tuberculoma are shown in Table 2.

Caseating solid granuloma is the most common type of tuberculoma [46]. This is highly cellular composed of compressed glial tissue and granulation tissue in the core accounting for marked T2 low signal [47]. T2 low signal of the rim in caseating granuloma with central liquefaction is due to collagen. Marked perilesional edema and mass effect are seen in the early stages of granuloma formation. Tuberculomas can be solitary or multiple. Multiple tuberculomas usually show conglomeration. Multiple tuberculomas in different stages may be present at the same time. PMRS is helpful in the diagnosis of tuberculomas. Prominent decrease in N-Acetyl Aspartate: Creatinine (NAA: Cr) and a modest decrease in N-Acetyl Aspartate: Choline (NAA: Cho) is typical. A large peak of lipids at 1.3 ppm is typical of tuberculous pathology [48]. The presence of lipid peak in PMRS is however a non-specific finding present in pathologies like histoplasmosis, lymphoma, glioma, and metastasis as well. Morales et al. [25] have proposed the singlet peak at 3.8 ppm (in long, intermediate as well as short TE) to be considered specific for tuberculomas and tuberculous abscesses. The assignment of the peak at 3.8 ppm is difficult but from analysis of Morales et al. [25]; guanidinoacetate (Gua) is a possibility.

Differential diagnosis of different tuberculous pathologies is shown in Fig. 1. Differentiation features of the lesions from tuberculous pathologies are listed in Table 3.

2) Disseminated tuberculomas (miliary tuberculomas) (Fig. 3A-3F)

Multiple T2 low or high signal intensity lesions of size <5 mm are scattered in cerebral parenchyma [14,26]. These lesions are seen in association with tuberculous leptomeningitis and are commonly seen in the pediatric age group. The lesions show intense homogeneous post-contrast enhancement. These lesions are more prominent in MT T1 weighted images and MT imaging helps to define disease load [57].

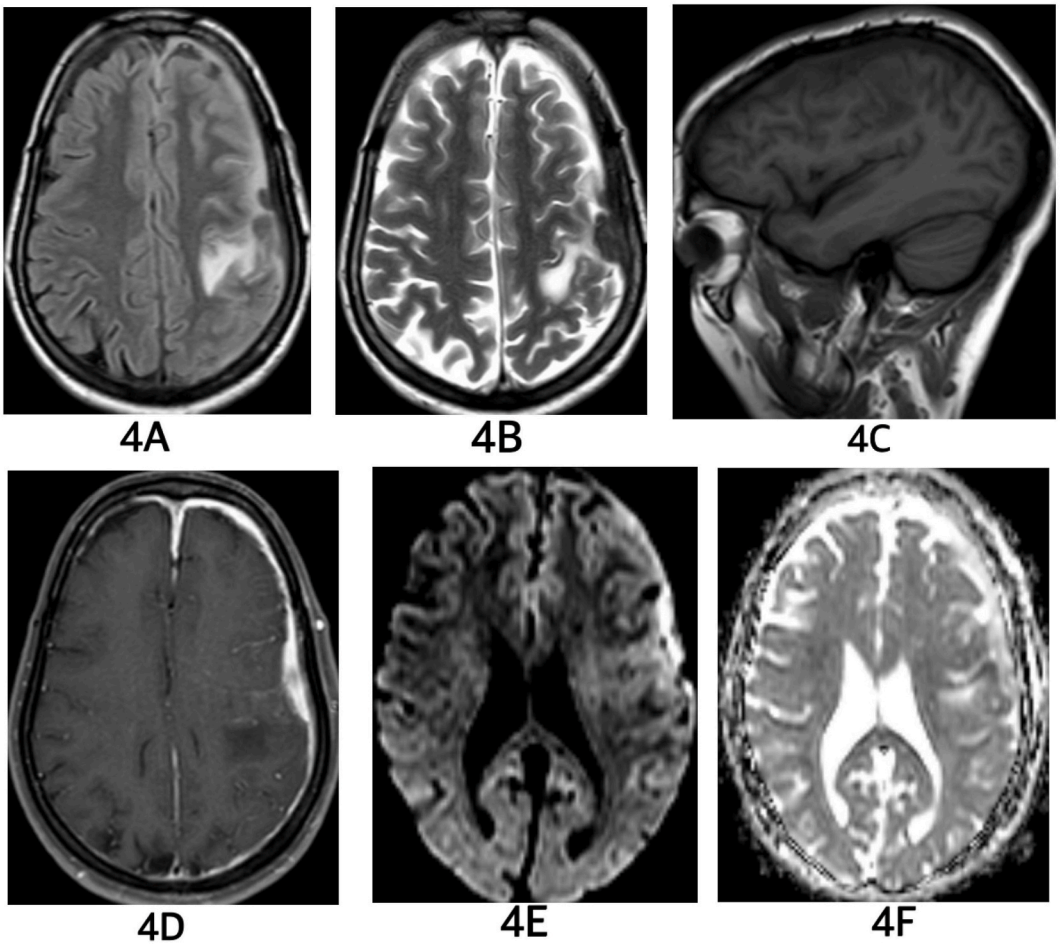

Fig. 4. MRI of a 54 years old male with HIV negative status showing pachymeningeal TBM. Axial FLAIR (4A) reveals diffuse pachymeningeal thickening with high signal in left cerebral hemisphere. Axial T2 (4B) shows similar findings. Sagittal T1 (4C) exhibits low signal of thickened pachymeninges. Axial PC T1 (4D) displays thickening and enhancement of meninges in left cerebral hemisphere, right frontal lobe, and along midline falx. Mild leptomeningeal enhancement is seen in left parietal lobe. Axial DWI and ADC images (4E, 4F) show patches of diffusion restriction in left parietal dura.

3) Tuberculous abscess (Fig. 8A-8F)

A tuberculous abscess is usually formed in elderly and immunocompromised patients. These are seen in 10 % of patients with CNS tuberculosis [58] and 20 % of patients with TB and HIV coinfection [14,59,60]. Tuberculous abscess is fairly common after solid organ transplant (SOT). In a review of tuberculosis after SOT, Singh et al. [61] reported that tuberculous abscess was present in 5 of 18 patients (28 %) with CNS TB. They are difficult to distinguish from the pyogenic abscess and caseating tuberculoma with central liquefaction. Clinically, the patients present with focal neurological deficits, features of raised intracranial pressure, and fever. According to Whitner criteria, to call any lesion a tuberculous abscess; there should be macroscopic evidence of pus in brain parenchyma; the abscess wall should have vascular granulation tissue containing acute and chronic inflammatory cells and tuberculous bacilli should be present in culture or histology [62]. In imaging, these lesions are usually large (>3 cm size), multiloculated with thin enhancing walls, demonstrate profound perilesional edema, and surrounding mass effect [5,26,53]. Contents of tuberculous abscess show low signal in T1 weighted images and high or mixed signal in T2 weighted images. Partial suppression may be seen in FLAIR. Central diffusion restriction is present in DWI due to the presence of pus [26]. Differentiation from pyogenic abscesses can be done with the help of PMRS. The presence of a lipid peak (at 1.3 ppm) and the absence of an amino acid peak on in vivo PMRS (at 0.9 ppm, 1.48 ppm, 1.92 ppm, 2.4 ppm, 2.4 ppm and 2.6 ppm) favor the diagnosis of tuberculous pseudo abscess [63,64]. Due to increased cellularity and liquefaction, a choline peak (at 3.22 ppm) might be present in addition to a lipid peak in tuberculous abscess [65]. MTR of a tuberculous abscess is less than a pyogenic abscess. It is important to differentiate tuberculous pseudo abscess from caseating granuloma in imaging since the management of both entities is different. Caseating granuloma is managed with antituberculous therapy and steroids. Tuberculous pseudo abscess however needs urgent surgical drainage. Large size (>3 cm), multiloculated appearance, presence of perilesional edema, mass effect, and central diffusion restriction favors the diagnosis of tuberculous pseudo abscess over

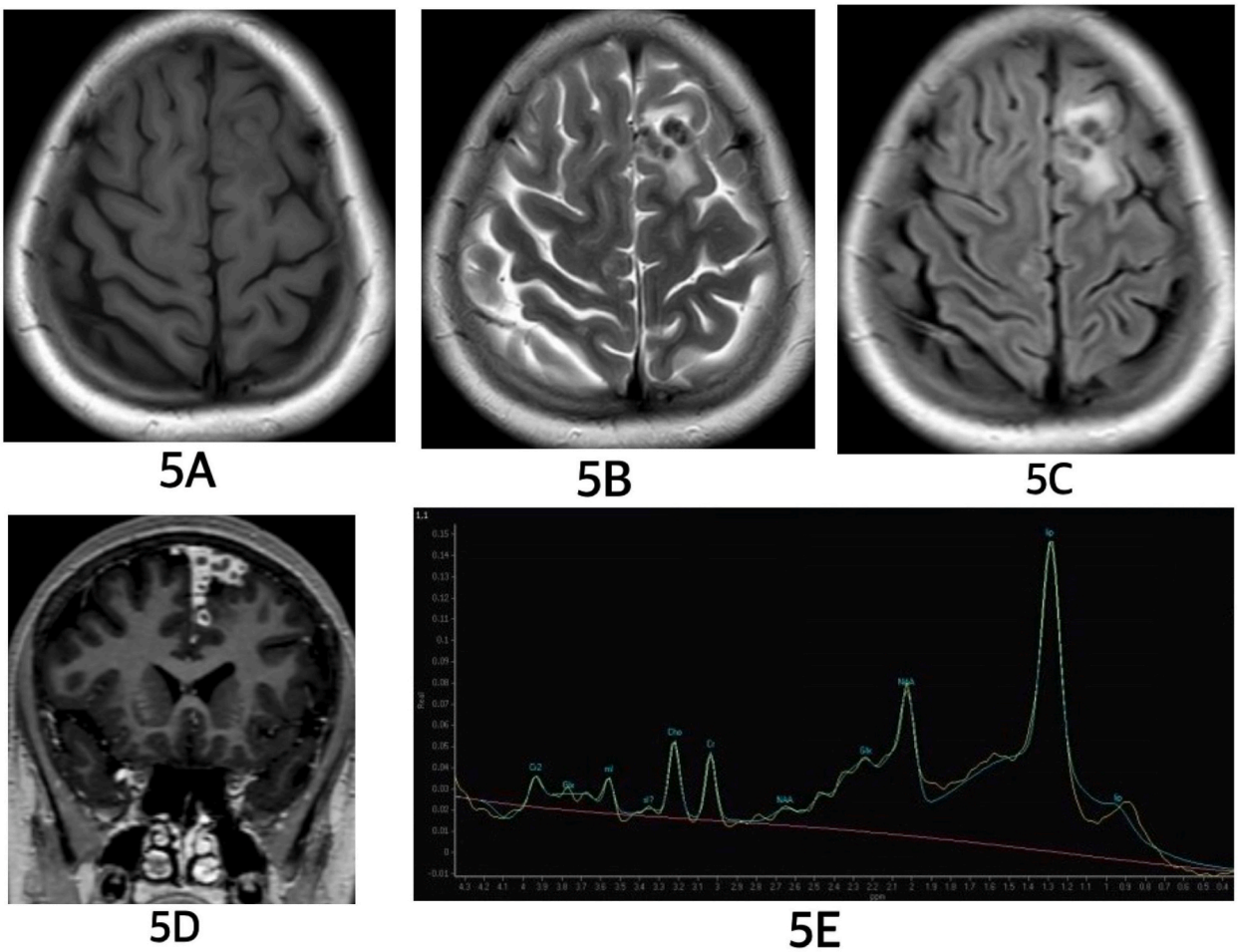

Fig. 5. MRI of a 25 years old female with HIV negative status showing tuberculomas and their MRS characteristics. Axial T1 (5A) shows low signal area in the left frontal lobe. Axial T2 (5B) displays conglomerated T2 low signal granulomas. Axial FLAIR (5C) shows tuberculous granulomas with perilesional edema. Coronal PC 3D T1 gradient echo (5D) displays multiple ring-enhancing lesions in the corresponding region. Single voxel short TE MRS (5E) of the lesion demonstrates a lipid peak at 1.3 ppm. Smaller NAA, Cho and Cr peaks are also seen.

caseating granuloma.

4) Tuberculous cerebritis

Isolated focal tuberculous cerebritis is very rare, almost exclusively seen in patients without AIDS (53). It usually occurs in association with tuberculous meningitis. It is defined as the focal area of cerebral parenchyma with edema and altered signal in MRI. The lesion shows a high signal in T2 and FLAIR and iso to low signal in T1 images. Pathologically, micro granulation is present with few bacilli and no caseation [26].

5) Tuberculous rhombencephalitis

It is a rare presentation of CNS tuberculosis affecting the hindbrain (brain stem and cerebellum). It accounts for 2 % of all rhombencephalitis cases. The prevalence of tuberculous rhombencephalitis is relatively high in patients with HIV/AIDS (66). It has a relatively poor prognosis and usually presents as focal neurological deficits in the form of cranial nerve palsies. Radiologically, it presents as tuberculomas in the midbrain or cerebellum with perilesional edema. Sometimes, only edema is present with no visible ring-enhancing lesions [5]. Features of raised intracranial pressure may be present due to hydrocephalus. Associated leptomeningeal enhancement of basal cistern is also present.

The differential diagnosis is rhombencephalitis of other infective and non-infective etiologies like Behçet's disease, Systemic Lupus Erythematosus (SLE), neurosarcoidosis, paraneoplastic syndrome, brain stem glioma, herpes and listeria [16]. MRS is of special importance in this case. Presence of a lipid peak at 1.3 ppm points towards tuberculous etiology.

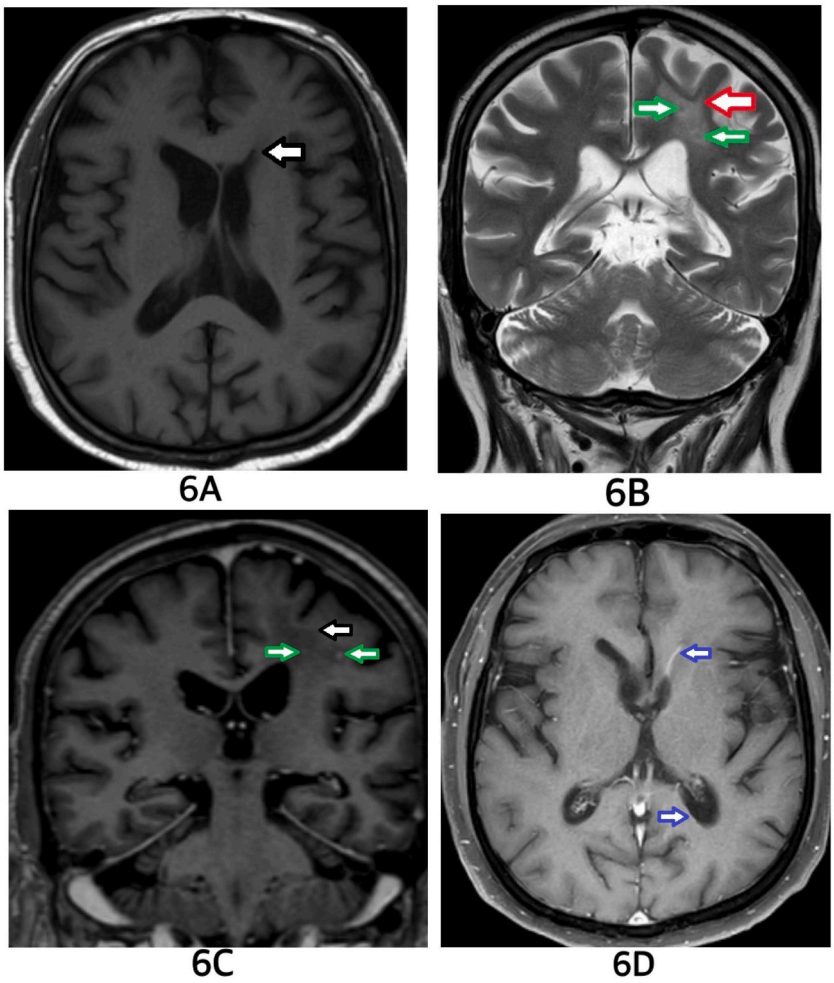

Fig. 6. MRI of a 58 years old male with HIV negative status showing tuberculous ependymitis. Axial T1 (6A) shows effacement of the left frontal horn (black arrow). Coronal T2 (6B) displays ill-defined T2 high signal in periventricular white matter around the frontal horn (red arrow), with tiny T2 low signal lesions (green arrow). Coronal PC 3D T1 gradient echo (6C) shows subtle enhancement of the T2 low signal lesions (green arrow). Axial PC T1 gradient echo (6D) reveals enhancement of the ependyma in the left frontal horn and subtle enhancement in the left occipital horn (blue arrow). (For interpretation of the references to colour in this figure legend, the reader is referred to the Web version of this article.)

6) Tuberculous encephalopathy

Tuberculous encephalopathy is seen in infants and children. It occurs because of a type IV hypersensitivity reaction to tuberculous protein mediated by the T lymphocytes. Pathologically, there is a loss of myelin, decreased oligodendroglia, and an increase in astrocytes in the brain resulting in extensive white matter injury. The child presents with seizure, altered sensorium, and stupor without signs of meningitis. Radiologically, diffuse white matter edema is seen in the form of patchy or diffuse T2 hyperintensity [66]. Diffusion restriction is not present. Patchy, subtle white matter enhancement may be seen in post-contrast images. Acute disseminated encephalomyelitis is a differential diagnosis. The prognosis is poor with death occurring within 1–2 months of onset despite antitubercular therapy [53].

6. Spinal tuberculosis (Fig. 9A-9D)

Spinal tuberculosis can be seen in one of three forms, i.e. extradural (64 %), intramedullary (8 %) or intradural extramedullary (1 %) form [1]. Extradural form is also called Pott's spine. It is the most common cause of paraplegia in any age group [67]. In this form, there is osteomyelitis of vertebral body and intervertebral discitis [68]. According to the site of involvement, Pott's spine can be classified as paradiscal, anterior, central, posterior and synovial types [53]. Paradiscal involvement occurs in hematogenous spread through arteries. Since discs are poor in arterial supply, they are often spared. Involvement of anterior part of vertebral body occurs if there is subligamentous spread of the disease along anterior longitudinal ligament. Skip lesions are not uncommon. Lumbar spine is most commonly involved [69]. There might be paraspinal extension of the disease with paraspinal collection. Subdural and epidural

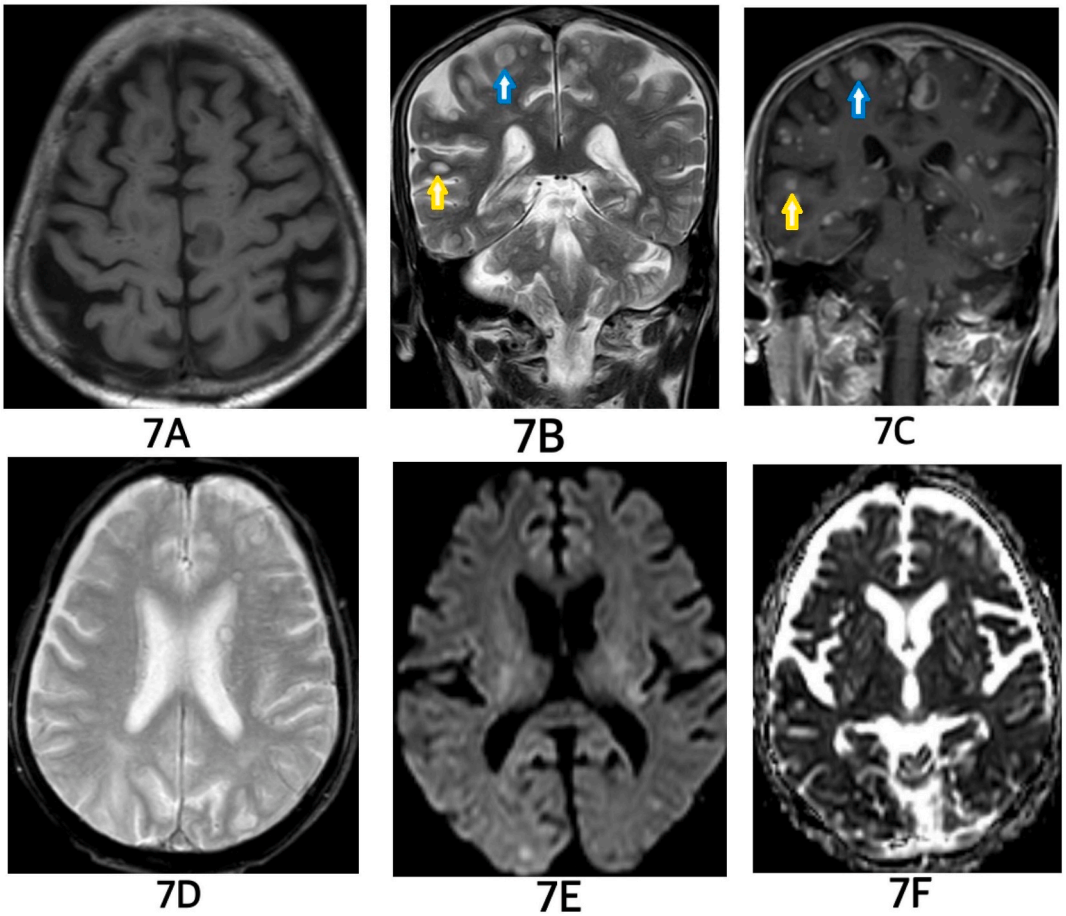

Fig. 7. MRI of a 40 years old male with HIV negative status showing multiple tuberculomas in different stages. Axial T1 (7A) shows well-defined low signal lesions in bilateral high parietal lobes. Coronal T2 (7B) displays multiple T2 low signal (yellow arrow) and high signal (blue arrow) lesions, indicating caseating solid and non-caseating tuberculomas. Coronal PC T1 gradient echo (7C) shows homogeneous disc enhancement in both types of lesions. Axial GRE T2* (7D), axial DWI (7E), and ADC (7F) images show no obvious abnormalities. (For interpretation of the references to colour in this figure legend, the reader is referred to the Web version of this article.)

Table 3
Differentiating features of tuberculous pathologies and their differentials.

Pyogenic/fungal/viral meningitis	Neurocysticercosis (NCC)	Pyogenic/Fungal brain abscess	Glioma	CNS lymphoma	Bain metastasis
• Amino acid and trehalose peaks, respectively, in pyogenic and fungal meningitis in PMRS [49]. • The magnetization transfer ratio (MTR) is higher in fungal and pyogenic meningitis but lower in viral meningitis compared to tuberculous meningitis [50].	• Thin-walled, high signal lesion in T2 with an eccentric T2 low signal scolex. • Succinate or acetate peak in MRS [51]. • Absence of lipid peak in MRS.	Pyogenic Abscess: • Cytosolic amino acid peak in MRS [49]. • Central diffusion restriction. Fungal Abscess: • Trehalose peak in MRS. • Crenated margin, intracavitary projections. • Diffusion restriction in margin and projections [49].	Glioma: • Choline peak in MRS. • Higher Cho/Cr and Cho/NAA ratios [52]. • Lower ADC values. • Irregular or nodular blooming in SWI [53]. Complete peripheral blooming in SWI is often seen in tuberculoma [51].	• Low signal In T2 • Diffusion restriction. • Choline peak in PMRS [54,55]. • Absence of lipid peak in MRS [55].	Brain Metastasis: • Choline peak in MRS [56]. • Higher Cho/Cr ratio. • Hemorrhage common. • Irregular or nodular blooming in SWI [53]. .

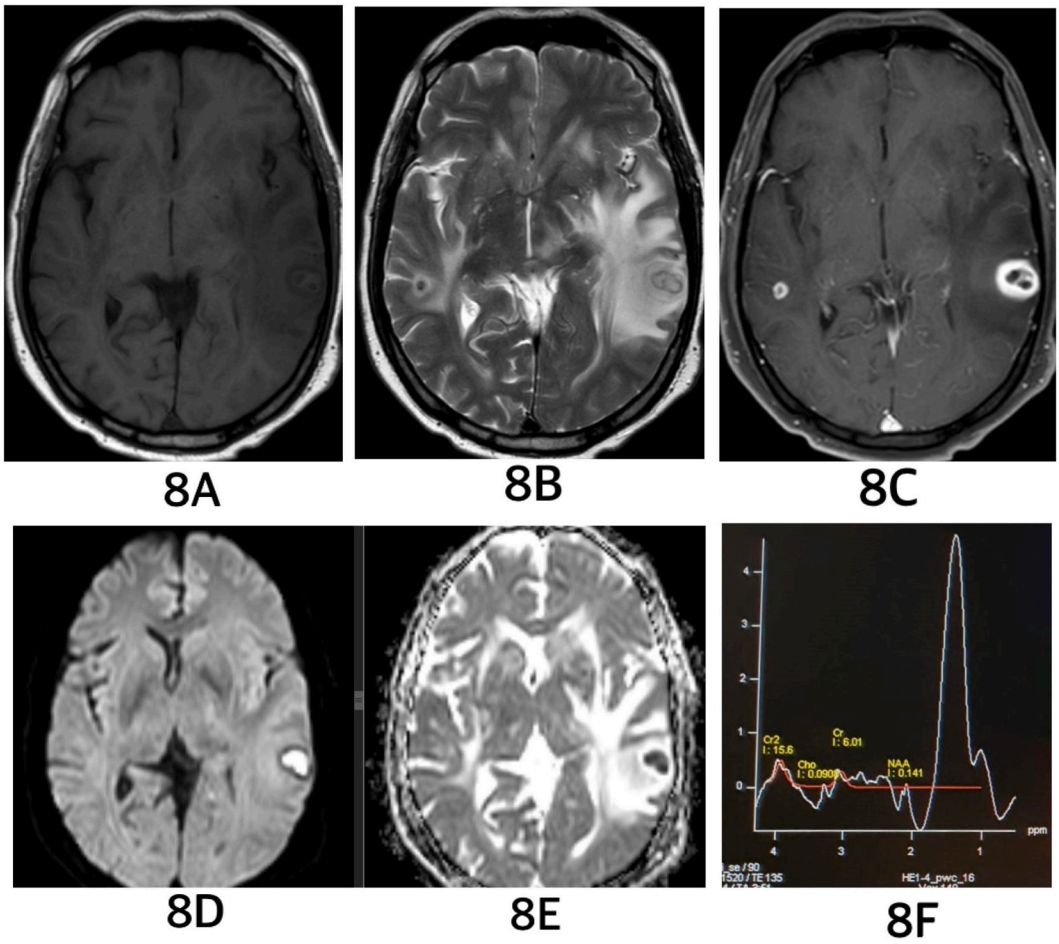

Fig. 8. MRI of a 42 years old female with HIV negative status showing multiple tuberculomas and tuberculous abscesses. Axial T1 (8A) and T2 (8B) show a lobulated T1 low signal, T2 high signal lesion with perilesional edema in the left temporal lobe and a T1/T2 low signal oval lesion in the right temporal lobe. Axial PC T1 (8C) displays ring enhancement in the lesions in both temporal lobes. DWI and ADC (8D) show central diffusion restriction in the left temporal lobe lesion. Single voxel PMRS (8E) from a T2 high signal lesion in the left temporal lobe reveals a lipid peak at 1.3 ppm. It is in contrast to pyogenic abscess, which displays cytosolic amino acid peaks at 0.9 ppm (valine, leucine and isoleucine), 1.48 ppm (alanine), 1.92 ppm (acetate), 2.4 ppm (succinate) and 2.6 ppm (aspartate).

abscess maybe present compressing the spinal cord and nerve roots. Because of contagious dissemination, spondylodiscitis can evolve to meningitis, intraspinal tuberculoma, radiculomyelitis (which can be late manifestation of the disease), myelitis, and/or arachnoiditis [69,70]. The infection spreads along the spinal nerve roots with enhancement along them. There might be associated cord edema. Cervical and dorsal spine are the most common sites of involvement in tuberculous myelitis [71]. The most common presentation is paraparesis. Tuberculous myelitis might result cavity formation and pus collection in the cord [72,73]. Although arachnoiditis can be present throughout the subarachnoid space, it is most frequently identified in the lumbar region and along the cauda equina, characterized by inflammation of neural roots and meninges.

There are 3 patterns of inflammation [74].

a) Type I: nerve roots are clumped together and distorted
b) Type II: nerve roots adherent to the theca, with the classical “empty thecal sac sign"
c) Type III: a single soft tissue mass centered within the spinal cord, consisting of roots, and theca.

MRI findings include loculated arachnoid cysts, intradural contrast enhancement, loss of the normal contour of the spine and an abnormal configuration of nerve roots as previously described. Arachnoiditis, CSF loculations maybe the additional findings. Syrinx maybe formed as sequalae of the infection.

Transverse myelitis (TM) or longitudinal extensive TM (LETM) manifest clinically by limb weakness, sensation abnormalities, and sphincter dysfunction. On MRI, findings of TM or LETM include T1-WI iso or low signal with correspondent poorly delineated T2-WI high signal and variable contrast-enhancement patterns [75]. The most important difference between TM and LETM is the

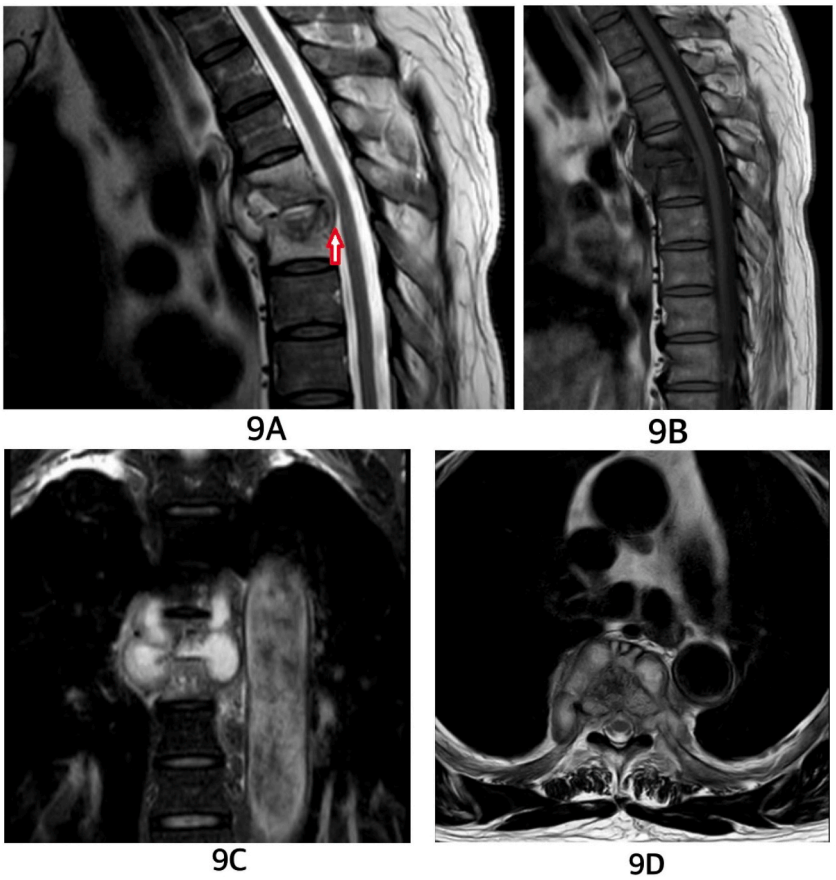

Fig. 9. MRI of a 28 years old male with HIV negative status showing Pott's spine involving D5-D6 intervertebral disc and vertebrae. Sagittal T2 (9A), T1 (9B), coronal STIR (9C) and axial T2 (9D) images reveal reduced disc height, altered vertebrae signal, and paravertebral collection (red arrow in 9A). (For interpretation of the references to colour in this figure legend, the reader is referred to the Web version of this article.)

cranio-caudal extension of the lesions (more than 3 vertebral bodies for LETM and less than 3 for TM). Both TM and LETM are rare presentations of neurotuberculosis, but TM is more related to this diagnosis than LETM, especially when associated to cerebral or systemic disseminated disease. On the other hand, LETM is more related to autoimmune diseases, such as neuromyelitis Optica spectrum disorders [76].

Spinal intramedullary tuberculoma occurs in 2: 100,000 cases of tuberculosis and in 2 % of all cases of neurotuberculosis, appearing as a thickened spinal cord with oval lesions. The lesions demonstrate low signal in T1 images, with a "target sign" on T2 images and an irregular peripheric enhancement after contrast administration [76].

7. Miscellaneous forms of CNS TB

1) **Tuberculous Hypophysitis**: It is a rare form of tuberculosis. There is diffuse enlargement of pituitary gland with thickened enhancing pituitary stalk [77]. Differential diagnosis includes eosinophilic granuloma, neurosarcoidosis, germinoma, syphilis etc.
2) **Orbital Tuberculosis:** This rare form of tuberculous infection is seen in pediatric age group and patients with HIV. Uveitis and chorioretinitis are the most common presentation. In imaging, unilateral enhancing choroidal lesion is seen [78]. In advanced form, there might be preseptal soft tissue stranding or collection. There might be inflammation of lacrimal gland with sclerosis/erosion of bony orbit. Orbital involvement is usually unilateral.
3) **Tuberculous otitis media and temporal bone tuberculosis:** This uncommon presentation is also seen in pediatric age group and present as chronic suppurative osteomyelitis. In imaging, inflammation, pus, sinus tracts are seen in middle and external ear and mastoid air cells. Painful otorrhea is seen. There might be erosion/sclerosis of adjoining temporal bone [79].
4) **Tuberculous osteomyelitis of calvarial bone:** This is a rare condition. Frontal and parietal bones are involved rather than other calvaria. Punched out lesion or erosion of the involved bone is seen [80].
5) **Tuberculous osteomyelitis of base of skull:** This is also a rare form of tuberculosis. Enhancing ill-defined soft tissue lesion may be present with erosion of skull base. Surrounding pus collection maybe present. The condition usually presents as cranial neuropathies [81].

8. Complications of CNS tuberculosis

Complications of CNS tuberculosis include hydrocephalus, vasculitis (arterial as well as venous), persistent neurological deficits, and cranial neuropathies. Arterial vasculitis may lead to infarction. Vasculitis involving cortical veins and dural venous sinus, though rare may result in cortical venous thrombosis, dural sinus thrombosis, and venous infarcts [26]. In the spine, syrinx may be formed. Pott's spine results in pathological fractures and deformities of the spine.

9. Paradoxical reactions following treatment

It is characterized by the worsening of pre-existing tuberculous lesions or the appearance of new tuberculous lesions following the initiation of treatment. This phenomenon occurs in about one-third of patients undergoing treatment [82]. Predictors for paradoxical reaction include female gender, immunocompromised status, and a shorter duration of treatment. Knowledge of paradoxical reactions following treatment prevents incorrect conclusions about the disease, such as treatment failure, drug resistance, drug toxicity, or an alternative diagnosis [83]. Paradoxical reactions can manifest as the worsening of hydrocephalus, optochiasmatic arachnoiditis, spinal arachnoiditis, and paradoxical worsening of cerebrospinal fluid (CSF) findings. In MRI, there is a worsening of findings compared to pre-treatment MRI. There might be an increase in basal exudates, an increase in the size or number of tuberculomas/tuberculous abscesses, or the appearance of new tuberculomas/tuberculous abscesses. Additionally, there may be an increase in perilesional edema, the development of new infarcts, and ventriculomegaly [84].

Source of funding

None.

Data availability statement

Data associated with this study is not available in public repository because this is a review article and no original data have been used.

CRediT authorship contribution statement

Prajwal Dahal: Visualization, Supervision, Methodology, Investigation, Formal analysis, Conceptualization. **Sabina Parajuli:** Writing – review & editing, Software, Resources.

Declaration of competing interest

The authors declare that they have no known competing financial interests or personal relationships that could have appeared to influence the work reported in this paper.

References

[1] V. Chaudhary, S. Bano, U.C. Garga, Central nervous system tuberculosis: an imaging perspective, Can. Assoc. Radiol. J. 68 (2) (2017 May) 161–170, https://doi.org/10.1016/j.carj.2016.10.007.
[2] J.M. Leonard, Central nervous system tuberculosis, Microbiol. Spectr. 5 (2) (2017 Mar), https://doi.org/10.1128/microbiolspec.TNMI7-0044-2017. PMID: 28281443.
[3] N. Adhikari, R.B. Bhattarai, R. Basnet, L.R. Joshi, B.S. Tinkari, A. Thapa, et al., Prevalence and associated risk factors for tuberculosis among people living with HIV in Nepal. Mahapatra B, PLoS One 17 (1) (2022 Jan 28) e0262720, https://doi.org/10.1371/journal.pone.0262720.
[4] A. Baloji, R.G. Ghasi, MRI in intracranial tuberculosis: have we seen it all? Clin. Imag. 68 (2020 Dec) 263–277, https://doi.org/10.1016/j.clinimag.2020.08.028. PMID: 32916507.
[5] G.D. Khatri, V. Krishnan, N. Antil, G. Saigal, Magnetic resonance imaging spectrum of intracranial tubercular lesions: one disease, many faces. pjr 83 (2018) 628–639, https://doi.org/10.5114/pjr.2018.81408. PMID: 30800191 PMCID: PMC6384409.
[6] M. Gupta, S. Munakomi, CNS tuberculosis, in: StatPearls [Internet], StatPearls Publishing, Treasure Island (FL), 2023 [cited 2023 Jul 31]./.
[7] [Internet], Table 23 | Reported TB in the US 2021 | Data & Statistics | TB, CDC, 2022 [cited 2023 Aug 1]. Available from: https://www.cdc.gov/tb/statistics/reports/2021/table23.htm.
[8] G. Thwaites, M. Fisher, C. Hemingway, G. Scott, T. Solomon, J. Innes, British Infection Society guidelines for the diagnosis and treatment of tuberculosis of the central nervous system in adults and children, J. Infect. 59 (3) (2009 Sep 1) 167–187, https://doi.org/10.1016/j.jinf.2009.06.011. PMID: 19643501.
[9] G.E. Marx, E.D. Chan, Tuberculous meningitis: diagnosis and treatment overview, Tuberc Res Treat. 2011 (2011) 798764, https://doi.org/10.1155/2011/798764. PMID: 22567269 PMCID: PMC3335590.
[10] M.A. Schaller, F. Wicke, C. Foerch, S. Weidauer, Central nervous system tuberculosis: etiology, clinical manifestations and neuroradiological features, Clin. Neuroradiol. 29 (1) (2019 Mar) 3–18, https://doi.org/10.1007/s00062-018-0726-9. PMID: 30225516.
[11] R.B. Rock, M. Olin, C.A. Baker, T.W. Molitor, P.K. Peterson, Central nervous system tuberculosis: pathogenesis and clinical aspects, Clin. Microbiol. Rev. 21 (2) (2008 Apr) 243–261, https://doi.org/10.1128/CMR.00042-07, table of contents.
[12] N. Be, K. Kim, W. Bishai, S. Jain, Pathogenesis of central nervous system tuberculosis, Curr. Mol. Med. 9 (2) (2009) 94–99, https://doi.org/10.2174/156652409787816555.
[13] A.G. Davis, U.K. Rohlwink, A. Proust, A.A. Figaji, R.J. Wilkinson, The pathogenesis of tuberculous meningitis, J. Leukoc. Biol. 105 (2) (2019 Feb) 267–280, https://doi.org/10.1002/JLB.MR0318-102R.
[14] A. Bernaerts, F.M. Vanhoenacker, P.M. Parizel, J.W.M. Van Goethem, R. Van Altena, A. Laridon, et al., Tuberculosis of the central nervous system: overview of neuroradiological findings, Eur. Radiol. 13 (8) (2003 Aug) 1876–1890, https://doi.org/10.1007/s00330-002-1608-7. PMID: 12942288.

[15] X. Chen, F. Chen, C. Liang, G. He, H. Chen, Y. Wu, Y. Chen, J. Shuai, Y. Yang, C. Dai, L. Cao, X. Wang, E. Cai, J. Wang, M. Wu, L. Zeng, J. Zhu, D. Hai, W. Pan, S. Pan, C. Zhang, S. Quan, F. Su, MRI advances in the imaging diagnosis of tuberculous meningitis: opportunities and innovations, Front. Microbiol. 14 (2023 Dec 11) 1308149, https://doi.org/10.3389/fmicb.2023.1308149. PMID: 38149270; PMCID: PMC10750405.
[16] R. Trivedi, S. Saksena, R.K. Gupta, Magnetic resonance imaging in central nervous system tuberculosis, Indian J. Radiol. Imag. 19 (4) (2009 Oct-Dec) 256–265, https://doi.org/10.4103/0971-3026.57205. PMID: 19881100; PMCID: PMC2797736.
[17] M. Modi, K. Sharma, S. Prabhakar, M.K. Goyal, A. Takkar, N. Sharma, A. Garg, S. Faisal, N. Khandelwal, P. Singh, J. Sachdeva, R. Shree, V. Rishi, V. Lal, Clinical and radiological predictors of outcome in tubercular meningitis: a prospective study of 209 patients, Clin. Neurol. Neurosurg. 161 (2017 Oct) 29–34, https://doi.org/10.1016/j.clineuro.2017.08.006. Epub 2017 Aug 18. PMID: 28843114.
[18] H. Botha, C. Ackerman, S. Candy, J.A. Carr, S. Griffith-Richards, K.J. Bateman, Reliability and diagnostic performance of CT imaging criteria in the diagnosis of tuberculous meningitis, PLoS One 7 (6) (2012) e38982, https://doi.org/10.1371/journal.pone.0038982. Epub 2012 Jun 29. PMID: 22768055; PMCID: PMC3387202.
[19] P. Kar, C. Raychaudhuri, Evaluation of role of CT scan and MRI in diagnosis of tuberculosis of brain and spine, Int. J. Sci. Res. 8 (12) (2019 Dec) 31–33, https://doi.org/10.36106/ijsr.
[20] R. Mushtaq, S. Arooj, U. Kalsoom, R. Raja, Role of contrast enhanced FLAIR MRI as a new tool in diagnosing tuberculous meningitis, PAFMJ [Internet] 70 (5) (2020 Oct. 30) 1310–1314 [cited 2024 Feb. 6].
[21] B. Jeevanandham, T. Kalyanpur, P. Gupta, M. Cherian, Comparison of post-contrast 3D- T 1 -MPRAGE, 3D- T 1 -SPACE and 3D- T 2 -FLAIR MR images in evaluation of meningeal abnormalities at 3-T MRI, BJR 90 (1074) (2017 Jun) 20160834, https://doi.org/10.1259/bjr.20160834. PMID: 28375660 PMCID: PMC5602177.
[22] S. Mangalore, S. Desai, A. Mahadevan, J.M.E. Kovoor, L.M.K. Vasudev, A.B. Tally, et al., Cerebral tubercular thrombophlebitis presenting as venous infarct: magnetic resonance imaging and pathologic correlation, Ann. Indian Acad. Neurol. 17 (1) (2014) 130–134, https://doi.org/10.4103/0972-2327.128587.
[23] I.K. Sharawat, D. Bhattacharya, L. Saini, P. Singh, Multiple cerebral sinus venous thrombosis and venous infarct: rare complication of tuberculous meningitis in a child, BMJ Case Rep. 12 (7) (2019 Jul 22) e231419, https://doi.org/10.1136/bcr-2019-231419.
[24] S. Kumar, M. Gutch, Advanced magnetic resonance imaging techniques in tuberculous meningitis, Adv. Biomed. Res. 9 (1) (2020) 20, https://doi.org/10.4103/abr.abr_222_19.
[25] H. Morales, D. Alfaro, C. Martinot, N. Fayed, M. Gaskill-Shipley, MR spectroscopy of intracranial tuberculomas: a singlet peak at 3.8 ppm as potential marker to differentiate them from malignant tumors, NeuroRadiol. J. 28 (3) (2015 Jun) 294–302, https://doi.org/10.1177/1971400915592077. PMID: 26246099 PMCID: PMC4757282.
[26] Taheri M. Sanei, M.A. Karimi, H. Haghighatkhah, R. Pourghorban, M. Samadian, H. Delavar Kasmaei, Central nervous system tuberculosis: an imaging-focused review of a reemerging disease, Radiol. Res. Pract. 2015 (2015) 1–8, https://doi.org/10.1155/2015/202806. PMID: 25653877 PMCID: PMC4306383.
[27] L.M. Feitoza, V.M. Jarry, M.C. Ramos, F. Reis, High-resolution vessel wall MRI as a complementary investigation for CNS tuberculosis, Can. J. Neurol. Sci. 48 (5) (2021 Sep) 717–718, https://doi.org/10.1017/cjn.2020.265. Epub 2020 Dec 4. PMID: 33272344.
[28] N. Choudhary, S. Vyas, M. Modi, S. Raj, A. Kumar, N. Sankhyan, R. Suthar, A.G. Saini, M.K. Goyal, C.K. Ahuja, P. Singh, MR vessel wall imaging in tubercular meningitis, Neuroradiology 63 (10) (2021 Oct) 1627–1634, https://doi.org/10.1007/s00234-021-02678-y. Epub 2021 Feb 27. PMID: 33638692.
[29] S.H. Siddik, K.R. Ahmed, S.M. Hasan, Z. Tasnim, A. Zaman, R. Yasmin, et al., Spectrum of Presentation, Diagnosis, and Clinical Outcome of Central Nervous System Tuberculosis: A Case Series in Bangabandhu Sheikh Mujib Medical University, 2023, https://doi.org/10.21203/rs.3.rs-2778080/v1.
[30] C.A. Nelson, J.R. Zunt, Tuberculosis of the central nervous system in immunocompromised patients: HIV infection and solid organ transplant recipients, Clin. Infect. Dis. 53 (9) (2011 Nov) 915–926, https://doi.org/10.1093/cid/cir508. Epub 2011 Sep 29. PMID: 21960714; PMCID: PMC3218626.
[31] M. Ojha, S.R. Verma, S. Saran, M. Mital, P. Bansal, Imaging of CNS infections with Clinico-pathological correlation, Int. J. Contemp. Med. Res. [IJCMR] 6 (5) (2019), https://doi.org/10.21276/ijcmr.2019.6.5.23.
[32] A. Cherian, K.C. Ajitha, T. Iype, K.P. Divya, Neurotuberculosis: an update, Acta Neurol. Belg. 121 (1) (2021 Feb) 11–21, https://doi.org/10.1007/s13760-020-01575-0. PMID: 33400226.
[33] M.K. Sinha, R.K. Garg, H.K. Anuradha, A. Agarwal, A. Parihar, P.A. Mandhani, Paradoxical vision loss associated with optochiasmatic tuberculoma in tuberculous meningitis: a report of 8 patients, J. Infect. 60 (6) (2010 Jun) 458–466, https://doi.org/10.1016/j.jinf.2010.03.013. Epub 2010 Mar 25. PMID: 20346972.
[34] R.K. Garg, V. Paliwal, H.S. Malhotra, Tuberculous optochiasmatic arachnoiditis: a devastating form of tuberculous meningitis, Expert Rev. Anti Infect. Ther. 9 (9) (2011 Sep) 719–729, https://doi.org/10.1586/eri.11.93. PMID: 21905782.
[35] J.L. Dietemann, Bernardo R. Correia, A. Bogorin, M. Abu Eid, M. Koob, T. Nogueira, et al., [Normal and abnormal meningeal enhancement: MRI features], J. Radiol. 86 (11) (2005 Nov) 1659–1683, https://doi.org/10.1016/s0221-0363(05)81507-0. PMID: 16269979.
[36] J.G. Smirniotopoulos, F.M. Murphy, E.J. Rushing, J.H. Rees, J.W. Schroeder, Patterns of contrast enhancement in the brain and meninges, Radiographics 27 (2) (2007 Mar) 525–551, https://doi.org/10.1148/rg.272065155. PMID: 17374867.
[37] S.K. Guler, N. Güneş, B.G. Cokal, T. Yoldas, Tuberculous ventriculitis as a relapse following central nervous system tuberculoma, Neurol. Sci. 36 (1) (2015 Jan 1) 167–169, https://doi.org/10.1007/s10072-014-1861-y. PMID: 24985158.
[38] R.L. He, Y. Liu, Q. Tan, L. Wang, The rare manifestations in tuberculous meningoencephalitis: a review of available literature, Ann. Med. 55 (1) (2023 Dec) 342–347, https://doi.org/10.1080/07853890.2022.2164348. PMID: 36598144; PMCID: PMC9828632.
[39] U.K. Misra, J. Kalita, P.K. Maurya, Stroke in tuberculous meningitis, J. Neurol. Sci. 303 (1–2) (2011 Apr 15) 22–30, https://doi.org/10.1016/j.jns.2010.12.015. Epub 2011 Jan 26. PMID: 21272895.
[40] D. Lyndon, J.A. Lansley, J. Evanson, A.S. Krishnan, Dural masses: meningiomas and their mimics, Insights Imaging 10 (1) (2019 Feb 6) 11, https://doi.org/10.1186/s13244-019-0697-7. PMID: 30725238; PMCID: PMC6365311.
[41] T.B. Matias, R.A. Cordeiro, J.A. Duarte, V.M. de Jarry, S. Appenzeller, L. Villarinho, F. Reis, Immune-mediated hypertrophic pachymeningitis and its mimickers: magnetic resonance imaging findings, Acad. Radiol. 30 (11) (2023 Nov) 2696–2706, https://doi.org/10.1016/j.acra.2023.01.017. Epub 2023 Mar 6. PMID: 36882352.
[42] D. Muzumdar, R. Vedantam, D. Chandrashekhar, Tuberculosis of the central nervous system in children, Childs Nerv. Syst 34 (10) (2018 Oct) 1925–1935, https://doi.org/10.1007/s00381-018-3884-9. PMID: 29978252.
[43] D. Patkar, J. Narang, R. Yanamandala, M. Lawande, G.V. Shah, Central nervous system tuberculosis: pathophysiology and imaging findings, Neuroimaging Clin. 22 (4) (2012 Nov 1) 677–705, https://doi.org/10.1016/j.nic.2012.05.006. PMID: 23122262.
[44] H. Ma, Y. Liu, C. Zhuang, Y. Shen, R. Wu, Clinical features and MRI findings of intracranial tuberculomas, Radiol. Infect. Dis. 5 (4) (2018 Dec) 154–159, https://doi.org/10.1016/j.jrid.2018.10.001.
[45] R.K. Gupta, S. Kumar, Central nervous system tuberculosis, Neuroimaging Clin. 21 (4) (2011 Nov) 795–814, https://doi.org/10.1016/j.nic.2011.07.004. PMID: 22032500.
[46] A.R. DeLance, M. Safaee, M.C. Oh, A.J. Clark, G. Kaur, M.Z. Sun, et al., Tuberculoma of the central nervous system, J. Clin. Neurosci. 20 (10) (2013 Oct 1) 1333–1341, https://doi.org/10.1016/j.jocn.2013.01.008. PMID: 23768968.
[47] M. Azeemuddin, A. Alvi, R. Sayani, M.K. Khan, S. Farooq, M.A. Beg, et al., Neuroimaging findings in tuberculosis: a single-center experience in 559 cases, J. Neuroimaging 29 (5) (2019 Sep) 657–668, https://doi.org/10.1111/jon.12627. PMID: 31115112.
[48] M. Gutch, N. Jain, A. Agrawal, A. Modi, MR spectroscopy in tuberculoma of brain, BMJ Case Rep. (2012), https://doi.org/10.1136/bcr.08.2011.4712.
[49] G. Luthra, A. Parihar, K. Nath, S. Jaiswal, K.N. Prasad, N. Husain, et al., Comparative evaluation of fungal, tubercular, and pyogenic brain abscesses with conventional and diffusion MR imaging and proton MR spectroscopy, AJNR Am J Neuroradiol 28 (7) (2007 Aug) 1332–1338, https://doi.org/10.3174/ajnr.A0548. PMID: 17698537 PMCID: PMC7977670.
[50] M.H. Pui, M.N. Ahmad, Magnetization transfer imaging diagnosis of intracranial tuberculomas, Neuroradiology 44 (3) (2002 Mar) 210–215, https://doi.org/10.1007/s002340100693. PMID: 11942374.

[51] R.P. Maheshwarappa, C. Agrawal, J. Bansal, Tuberculoma versus neurocysticercosis: can magnetic resonance spectroscopy and diffusion weighted imaging solve the diagnostic conundrum, J. Clin. Diagn. Res. (2019), https://doi.org/10.7860/jcdr/2019/41334.12957.

[52] J. Peng, Y. Ouyang, W.D. Fang, T.Y. Luo, Y.M. Li, F.J. Lv, et al., Differentiation of intracranial tuberculomas and high grade gliomas using proton MR spectroscopy and diffusion MR imaging, Eur. J. Radiol. 81 (12) (2012 Dec) 4057–4063, https://doi.org/10.1016/j.ejrad.2012.06.005. PMID: 22749802.

[53] A.H. Parry, A.H. Wani, F.A. Shaheen, A.A. Wani, I. Feroz, M. Ilyas, Evaluation of intracranial tuberculomas using diffusion-weighted imaging (DWI), magnetic resonance spectroscopy (MRS) and susceptibility weighted imaging (SWI), BJR 91 (1091) (2018 Nov) 20180342, https://doi.org/10.1259/bjr.20180342. PMID: 29987985 PMCID: PMC6475934.

[54] G. Cheng, J. Zhang, Imaging features (CT, MRI, MRS, and PET/CT) of primary central nervous system lymphoma in immunocompetent patients, Neurol. Sci. 40 (3) (2019 Mar) 535–542, https://doi.org/10.1007/s10072-018-3669-7. Epub 2018 Dec 22. PMID: 30580380; PMCID: PMC6433804.

[55] J. Li, M. Xue, S. Yan, C. Guan, R. Xie, B. Chen, A comparative study of multimodal magnetic resonance in the differential diagnosis of acquired immune deficiency syndrome related primary central nervous system lymphoma and infection, BMC Infect. Dis. 21 (1) (2021 Feb 10) 165, https://doi.org/10.1186/s12879-021-05779-4. PMID: 33568094; PMCID: PMC7874668.

[56] C.K. Onyambu, M.N. Wajihi, A.O. Odhiambo, Clinical application of magnetic resonance spectroscopy in diagnosis of intracranial mass lesions, Radiol. Res. Pract. 2021 (2021 Feb 18) 6673585, https://doi.org/10.1155/2021/6673585. PMID: 38173977; PMCID: PMC10763544.

[57] P. Janse van Rensburg, S. Andronikou, R. van Toorn, M. Pienaar, Magnetic resonance imaging of miliary tuberculosis of the central nervous system in children with tuberculous meningitis, Pediatr. Radiol. 38 (12) (2008 Dec) 1306–1313, https://doi.org/10.1007/s00247-008-1028-1. PMID: 18931835.

[58] C. Torres, R. Riascos, R. Figueroa, R.K. Gupta, Central nervous system tuberculosis, Top. Magn. Reson. Imag. 23 (3) (2014 Jun) 173–189, https://doi.org/10.1097/RMR.0000000000000023. PMID: 24887691.

[59] S. Saxena, M. Prakash, S. Kumar, R.K. Gupta, Comparative evaluation of magnetization transfer contrast and fluid attenuated inversion recovery sequences in brain tuberculoma, Clin. Radiol. 60 (7) (2005 Jul) 787–793, https://doi.org/10.1016/j.crad.2004.09.016. PMID: 15978890.

[60] J.E. Vidal, ACP de Oliveira, F.B. Filho, R.S. Nogueira, R.F. Dauar, A.G. Leite, et al., Tuberculous brain abscess in AIDS patients: report of three cases and literature review, Int. J. Infect. Dis. 9 (4) (2005 Jul 1) 201–207, https://doi.org/10.1016/j.ijid.2004.06.010. PMID: 15964538.

[61] N. Singh, D.L. Paterson, Mycobacterium tuberculosis infection in solid-organ transplant recipients: impact and implications for management, Clin. Infect. Dis. 27 (5) (1998 Nov) 1266–1277, https://doi.org/10.1086/514993. PMID: 9827281.

[62] B.L. Fatoumata, S.I. Sory, C.F. Abass, D.H. Bachir, A.H. Ghislain, C.A. Youssouf, et al., Cerebral abscesses of tuberculosis origin: study of 8 cases at the university hospital of Conakry, Egypt. J. Neurosurg. 35 (1) (2020), https://doi.org/10.1186/s41984-020-00090-x.

[63] R.K. Gupta, D.K. Vatsal, N. Husain, S. Chawla, K.N. Prasad, R. Roy, R. Kumar, D. Jha, M. Husain, Differentiation of tuberculous from pyogenic brain abscesses with in vivo proton MR spectroscopy and magnetization transfer MR imaging, AJNR Am J Neuroradiol 22 (8) (2001 Sep) 1503–1509. PMID: 11559497; PMCID: PMC7974561.

[64] M. Garg, R.K. Gupta, M. Husain, S. Chawla, J. Chawla, R. Kumar, S.B. Rao, M.K. Misra, K.N. Prasad, Brain abscesses: etiologic categorization with in vivo proton MR spectroscopy, Radiology 230 (2) (2004 Feb) 519–527, https://doi.org/10.1148/radiol.2302021317. Epub 2003 Dec 29. PMID: 14699181.

[65] P.N. Koffi, O. Ouambi, N. El Fatemi, R. El Maaquili, Tuberculome cérébral un challenge diagnostic: à propos d'un cas et mise au point [Cerebral tuberculoma a diagnostic challenge: case study and update], French, Pan Afr. Med. J. 32 (2019 Apr 10) 176, https://doi.org/10.11604/pamj.2019.32.176.16623. PMID: 31303945; PMCID: PMC6607260.

[66] D.R. Whitener, Tuberculous brain abscess. Report of a case and review of the literature, Arch. Neurol. 35 (3) (1978 Mar) 148–155, https://doi.org/10.1001/archneur.1978.00500270030007. PMID: 629659.

[67] G.L.O. Salvador, A.C.N. Basso, P.P. Barbieri, C.A. Leitao, B.C.A. Teixeira, A.C. Neto, Central nervous system and spinal cord tuberculosis: revisiting an important disease, Clin. Imag. 69 (2021 Jan) 158–168.

[68] L.R. Tomar, D.J. Shah, P. Agarwal, A. Rohatgi, C.S. Agrawal, Tubercular rhombencephalitis: a clinical challenge, Ann. Indian Acad. Neurol. 24 (6) (2021) 960–962, https://doi.org/10.1016/j.clinimag.2020.07.020. PMID: 32853843.

[69] R.K. Garg, Tuberculosis of the central nervous system, Postgrad. Med. 75 (881) (1999 Mar) 133–140, https://doi.org/10.1136/pgmj.75.881.133. PMID: 10448488; PMCID: PMC1741157.

[70] K. Lury, J.K. Smith, M. Castillo, Imaging of spinal infections, Semin. Roentgenol. 41 (4) (2006 Oct) 363–379, https://doi.org/10.1053/j.ro.2006.07.008. PMID: 17010695.

[71] E. Skoura, A. Zumla, J. Bomanji, Imaging in tuberculosis, Int. J. Infect. Dis. 32 (2015 Mar) 87–93, https://doi.org/10.1016/j.ijid.2014.12.007. PMID: 25809762.

[72] R.K. Garg, H.S. Malhotra, R. Gupta, Spinal cord involvement in tuberculous meningitis, Spinal Cord 53 (9) (2015 Sep) 649–657, https://doi.org/10.1038/sc.2015.58. Epub 2015 Apr 21. PMID: 25896347.

[73] R.K. Garg, D.S. Somvanshi, Spinal tuberculosis: a review, J. Spinal Cord Med. 34 (5) (2011) 440–454, https://doi.org/10.1179/2045772311Y.0000000023. PMID: 22118251; PMCID: PMC3184481.

[74] Ottaiano, A., & De Andrade Lourenção Freddi, T. (n.d.). "Sticky Spine": A Review of the Imaging Findings for Spinal Arachnoiditis. Neurographics, 12(3), 169–175. https://doi.org/10.3174/ng.2100062.

[75] M.I. Khan, R.K. Garg, I. Rizvi, H.S. Malhotra, N. Kumar, A. Jain, R. Verma, P.K. Sharma, S. Pandey, R. Uniyal, P. Jain, Tuberculous myelitis: a prospective follow-up study, Neurol. Sci. 43 (9) (2022 Sep) 5615–5624, https://doi.org/10.1007/s10072-022-06221-6. Epub 2022 Jun 23. PMID: 35739331; PMCID: PMC9225802.

[76] I.C. Miyoshi, A.H.N. de Toledo, F.V. Pereira, L.L. Villarinho, M. Dalaqua, J. de Ávila Duarte, F. Reis, Infectious myelitis, Semin. Ultrasound CT MR 44 (5) (2023 Oct) 424–435, https://doi.org/10.1053/j.sult.2023.03.015. Epub 2023 Apr 5. PMID: 37555684.

[77] I. Ates, B. Katipoglu, B. Copur, N. Yilmaz, A rare cause of hypophysitis: tuberculosis, Endocr. Regul. 51 (4) (2017 Oct 26) 213–215, https://doi.org/10.1515/enr-2017-0022. PMID: 29232189.

[78] M.G. Harisinghani, T.C. McLoud, J.A. Shepard, J.P. Ko, M.M. Shroff, P.R. Mueller, Tuberculosis from head to toe, quiz 528-9, 532, Radiographics 20 (2) (2000 Mar-Apr) 449–470, https://doi.org/10.1148/radiographics.20.2.g00mc12449. PMID: 10715343.

[79] M.H. Rho, D.W. Kim, S.S. Kim, Y.S. Sung, J.S. Kwon, S.W. Lee, Tuberculous otomastoiditis on high-resolution temporal bone CT: comparison with nontuberculous otomastoiditis with and without cholesteatoma, AJNR Am J Neuroradiol 28 (3) (2007 Mar) 493–496. PMID: 17353320; PMCID: PMC7977825.

[80] V.I. Sundar, J. Shekhawat, A. Gupta, V.D. Sinha, Post traumatic tubercular osteomyelitis of skull vault, J. Neurosci. Rural Pract. 4 (Suppl 1) (2013 Aug) S138–S141, https://doi.org/10.4103/0976-3147.116471. PMID: 24174787; PMCID: PMC3808049.

[81] Kumar, S., Kumar, A., Gadhavi, H., & Maheshwari, V. (n.d.). Tubercular skull base osteomyelitis in an immunocompetent individual: A rare entity". Interdiscip. Neurosurg., 24, 100816. https://doi.org/10.1016/j.inat.2020.100816.

[82] K.W. Kim, H.J. Kim, H.W. Kim, S.H. Kim, S.A. Lee, Y.S. Koo, Intractable tuberculous meningitis with paradoxical reactions treated by anti-tissue necrosis factor-α therapy, Neurol. Clin. Pract. 11 (4) (2021 Aug) e555–e557, https://doi.org/10.1212/CPJ.0000000000000946. PMID: 34484957; PMCID: PMC8382441.

[83] A.K. Singh, H.S. Malhotra, R.K. Garg, A. Jain, N. Kumar, N. Kohli, R. Verma, P.K. Sharma, Paradoxical reaction in tuberculous meningitis: presentation, predictors and impact on prognosis, BMC Infect. Dis. 16 (2016 Jun 21) 306, https://doi.org/10.1186/s12879-016-1625-9. PMID: 27329253; PMCID: PMC4915108.

[84] S.D.H.S. Perera, Paradoxical reaction to antitubercular treatment in a case of tuberculous meningitis, Cureus 15 (8) (2023 Aug 26) e44151, https://doi.org/10.7759/cureus.44151. PMID: 37753002; PMCID: PMC10519641.